Measurement of Transverse Spin Dependent Azimuthal Correlations of $\pi^+\pi^-$ in $p^\uparrow p$ Collisions at $\sqrt{s} = 200$ GeV at STAR

Babu Pokhrel[1], for the STAR Collaboration

[1] *Temple University, Philadelphia, PA, 19122, USA*

E-mail: babu.pokhrel@temple.edu

(Received January 13, 2022)

At the leading twist, the transversity distribution function, $h_1^q(x)$, where x is the longitudinal momentum fraction of the proton carried by quark q, encodes the transverse spin structure of the nucleon. Extraction of $h_1^q(x)$ is difficult because of its chiral-odd nature. In transversely polarized proton-proton collisions ($p^\uparrow p$), $h_1^q(x)$ can be coupled with another chiral-odd partner, a spin-dependent fragmentation function (FF). The resulting asymmetries in azimuthal correlations of di-hadron pairs directly probe $h_1^q(x)$. We report the measurement of di-pion ($\pi^+\pi^-$) correlation asymmetries in $p^\uparrow p$, which is sensitive to the valence quark transversity.

KEYWORDS: transversity, di-hadron correlation asymmetry, interference fragmentation function

1. Introduction

At the leading twist, the nucleon structure is fully described by three Parton Distribution Functions (PDFs): the unpolarized PDF, $f_1(x)$, the helicity PDF, $g_1(x)$, and the transversity PDF, $h_1^q(x)$, where x is the nucleon momentum fraction carried by partons. Although, $f_1(x)$ and $g_1(x)$ are reasonably well constrained by experimental data [1, 2], the knowledge of $h_1^q(x)$ is limited to the semi-inclusive deep inelastic scattering (SIDIS) and e^+e^- data [3]. This is because $h_1^q(x)$ is a chiral-odd object and it needs to be coupled with another chiral-odd partner to form a chiral-even cross section that is experimentally observable.

In polarized proton-proton collisions ($p^\uparrow p$), $h_1^q(x)$ can be coupled with chiral-odd spin-dependent fragmentation functions (FFs). Selecting oppositely charged di-hadron pairs in the final state involves the di-hadron interference FF (IFF). The coupling of $h_1^q(x)$ with the IFF results in experimentally measurable azimuthal correlation asymmetry, A_{UT}, which is sensitive to the quark $h_1^q(x)$.

2. Experiment and Dataset

The Relativistic Heavy-Ion Collider (RHIC) at Brookhaven National Laboratory (BNL) is capable of colliding bunched beams of polarized protons up to center-of-mass energy, $\sqrt{s}$, of 510 GeV. The Solenoidal Tracker At RHIC (STAR) is one of the major experiments, where the Time Projection Chamber (TPC) is the core detector that provides particle tracking and identification in the mid-pseudorapidity region ($-1 < \eta < 1$) and over the whole 2π range in azimuthal angle [4]. The time-of-flight detector (TOF) [5], with similar coverage as the TPC, improves the STAR's particle identification (PID) capability. The barrel electromagnetic calorimeter (BEMC) provides event triggering based on the energy depositions in its towers.

STAR firstly observed significant IFF asymmetry for $\pi^+\pi^-$ based on 2006 $p^\uparrow p$ data at $\sqrt{s}$ =

200 GeV [6], followed by the 2011 data at $\sqrt{s}$ = 500 GeV [7]. Current analysis is based on the $p^{\uparrow}p$ data at $\sqrt{s}$ = 200 GeV collected by STAR in the year 2015. This dataset corresponds to the integrated luminositiy of $\sim$ 52 pb^{-1} with the average beam polarization of $\sim$ 58%. It provides the most precise measurements of the IFF asymmetries in $p^{\uparrow}p$ at $\sqrt{s}$ = 200 GeV to date, especially at quark momentum fractions $0.1 < x < 0.3$.

3. Ananlysis

The IFF asymmetries for the $\pi^+\pi^-$ are extracted using the cross-ratio formula [8],

$$A_{UT} \cdot sin(\phi_{RS}) = \frac{1}{P} \cdot \frac{\sqrt{N^{\uparrow}(\phi_{RS})N^{\downarrow}(\phi_{RS}+\pi)} - \sqrt{N^{\downarrow}(\phi_{RS})N^{\uparrow}(\phi_{RS}+\pi)}}{\sqrt{N^{\uparrow}(\phi_{RS})N^{\downarrow}(\phi_{RS}+\pi)} + \sqrt{N^{\downarrow}(\phi_{RS})N^{\uparrow}(\phi_{RS}+\pi)}} \tag{1}$$

where, $N^{\uparrow(\downarrow)}$ is the number of exclusive $\pi^+\pi^-$ pairs, when the beam polarization is up(down). P is the average beam polarization. The definition of azimuthal angle $\phi_{RS} (= \phi_s - \phi_R)$ is illustrated in figure 1 [6], where ϕ_s is an angle between the polarization vector, $\vec{s}_a$, and the scattering plane, formed by the beam momentum vector, $\vec{p}_{beam}$, and the di-hadron momentum sum vector, $\vec{p}_h (= \vec{p}_{h,1} + \vec{p}_{h,2})$. ϕ_R is an angle between the scattering plane and the di-hadron plane, formed by two hadrons' momenta, $\vec{p}_{h,1}$, and $\vec{p}_{h,2}$. $\vec{R}(= \frac{1}{2}(\vec{p}_{h,1} - \vec{p}_{h,2}))$ is the relative momentum vector of the di-hadron system. Here, $\vec{p}_{h,1}$ is reserved for π^+ and $\vec{p}_{h,2}$ for π^-. This charge ordering is important, otherwise the direction of $\vec{R}$ is randomized resulting in diluted asymmetry. The mechanism of producing azimuthal correlations and its extraction from a theoretical point of view can be found in [9].

High-quality tracks associated with the event vertices within 60 cm along the beam direction from the nominal TPC center are used in this analysis. Each track is required to have transverse momentum $p_T > 1.5$ GeV/c and the distance of closest approach $dca < 1$ cm from the event vertex. Charged pions are identified by measuring their ionization energy loss, $\langle dE/dx \rangle$. Pions are selected by requiring a cut on the number of standard deviations of measured $\langle dE/dx \rangle$ from the expected pion energy loss, $-1 < n\sigma_\pi < 2$. The $\pi^\pm$ purity varies from 83% to 90% in $p_T^{\pi^+\pi^-}$ bins, 85% to 88% in $M_{inv}^{\pi^+\pi^-}$ bins, and 87% to 90% in $\eta^{\pi^+\pi^-}$ bins. However, $\pi^+\pi^-$ purity, which is the probability that both tracks in a pair are pions, ranges from 67% $\sim$ 80% over all kinematic bins.

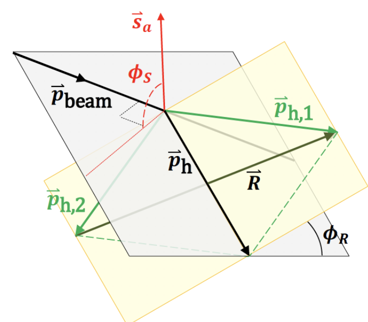

Fig. 1. Azimuthal angles in di-hadron system.

The $\pi^+\pi^-$ pairs are formed by selecting oppositely charged pion tracks and associated azimuthal angles are constructed as shown in figure 1. The π^+ and π^- tracks should be close enough in $\eta - \phi$ space ($\sqrt{(\eta^{\pi^+} - \eta^{\pi^-})^2 + (\phi^{\pi^+} - \phi^{\pi^-})^2} < 0.7$). The $\pi^+\pi^-$ yields are sorted based on the beam polarization direction ($\uparrow$ / $\downarrow$) in 16 ϕ_{RS} bins. The $\pi^+\pi^-$ correlation asymmetry, $A_{UT}^{sin(\phi_{RS})}$, is then extracted from equation 1 as an amplitude of the sinusoidal fit over the range $[-\pi, 0]$. Analysis is performed for both polarized beams, the beam travelling clockwise (*blue*) and counterclockwise (*yellow*) in the RHIC ring, separately. The final result is the weighted average of both.

Two different types of systematic effects are studied in this analysis: one includes the effect from the bias in the event triggering (*trigger bias*) and the other includes the effect related to the detector inefficiency on PID. To estimate the trigger bias effect, PYTHIA 6 [10] events are run through the STAR detector simulation implemented in GEANT 3 [11] and embedded into zero-bias events. The magnitude of the bias is determined by calculating the fraction of quark events at the detector level

(GEANT) and the particle level (PYTHIA) and taking a ratio between them. The size of the systematic effect related to the PID is estimated using $\pi^+\pi^-$ impurity ($\sim 20\% - 33\%$) in the respective asymmetry bins. which is the dominant systematic uncertainty at this stage of the analysis.

4. Results

Figure 2 shows $A_{UT}^{sin(\phi_{RS})}$ as a function of the invariant mass of $\pi^+\pi^-$, $M_{inv}^{\pi^+\pi^-}$, in five $p_T^{\pi^+\pi^-}$ bins, which is the transverse momentum of $\pi^+\pi^-$ relative to the beam axis. Within each $p_T^{\pi^+\pi^-}$ bin, $A_{UT}^{sin(\phi_{RS})}$ is extracted in two pseudorapidity bins, $\eta^{\pi^+\pi^-} > 0$ (*forward*) and $\eta^{\pi^+\pi^-} < 0$ (*backward*). This shows the evolution of asymmetry signal with the $p_T^{\pi^+\pi^-}$ and $M_{inv}^{\pi^+\pi^-}$, simultaneously. Forward $A_{UT}^{sin(\phi_{RS})}$ signal has a resonance peak at $M_{inv}^{\pi^+\pi^-} \sim 0.8$ GeV/c^2, close to the $\rho-$meson mass, which becomes much stronger at higher $\langle p_T^{\pi^+\pi^-} \rangle$ bins. In the forward region, where high x quarks can be probed, this effect is expected due to the interference between $\pi^+\pi^-$ produced from different channels [12]. Backward asymmetries are small but non-zero. The backward region is dominated by the scattered quarks from the unpolarized beam and low x quarks from polarized beam, which carry less spin information, and therefore a smaller asymmetry signal is expected.

In figure 3, STAR 2015 $A_{UT}^{sin(\phi_{RS})}$ as a function of $M_{inv}^{\pi^+\pi^-}$, intrgrated over $p_T^{\pi^+\pi^-}$, in the forward region is compared with the STAR 2006 result and a theory curve (*gray band*), which is a fit to the SIDIS, e^+e^-, and STAR 2006 data from reference [13]. The uncertainty band is produced with the bootstrap method based on 600 replicas at 90% confidence level. Both STAR measurements are in good agreement with the theory with a significant resonance peak at $M_{inv}^{\pi^+\pi^-} \sim M_\rho$.

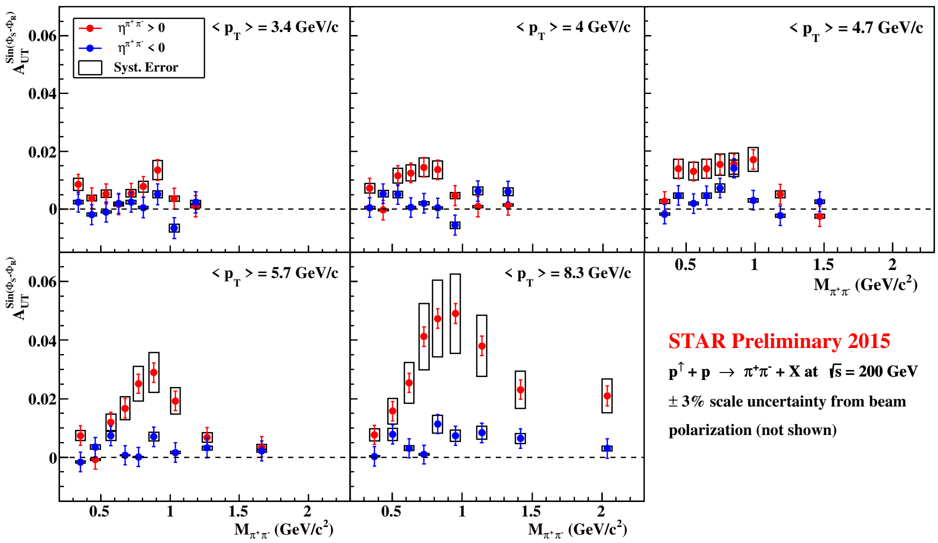

Fig. 2. $A_{UT}^{sin(\phi_{RS})}$ vs $M_{inv}^{\pi^+\pi^-}$, in five $p_T^{\pi^+\pi^-}$ bins in $\eta^{\pi^+\pi^-} > 0$ and $\eta^{\pi^+\pi^-} < 0$ regions. The value of $\langle p_T^{\pi^+\pi^-} \rangle$ for each of the transverse momentum bins is shown at the top right corner of each panel.

Figure 4 shows $A_{UT}^{sin(\phi_{RS})}$ as a function of $\eta^{\pi^+\pi^-}$, integrated over $M_{inv}^{\pi^+\pi^-}$ and $p_T^{\pi^+\pi^-}$ (*upper panel*). $< x >$, the average fractional proton momentum carried by a quark, and $< z >$, the average fractional quark energy carried by the $\pi^+\pi^-$ pair, are estimated from PYTHIA+GEANT simulation in the corresponding $\eta^{\pi^+\pi^-}$ bins and shown in the bottom panel. $A_{UT}^{sin(\phi_{RS})}$ increases linearly with $\eta^{\pi^+\pi^-}$ in the forward region while the backward asymmetry signal is small as expected. A strong correlation between the observed asymmetry and $< x >$ can be seen, where $< x >$ ranges from $\sim$ 0.1 to 0.22 from backward to forward $\eta^{\pi^+\pi^-}$. However, $< z >$ shows no clear dependence in $\eta^{\pi^+\pi^-}$ and its average is $\sim$ 0.46. The 2015 IFF results corroborate previous STAR measurements [6, 7].

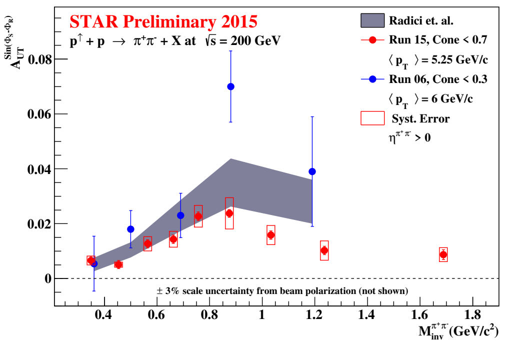

Fig. 3. $A_{UT}^{sin(\phi_{RS})}$ as a function of invarinat mass of two oppositely-charged pions, $M_{inv}^{\pi^+\pi^-}$, in $\eta^{\pi^+\pi^-}$>0 region, compared with the theoretical calculation from [13].

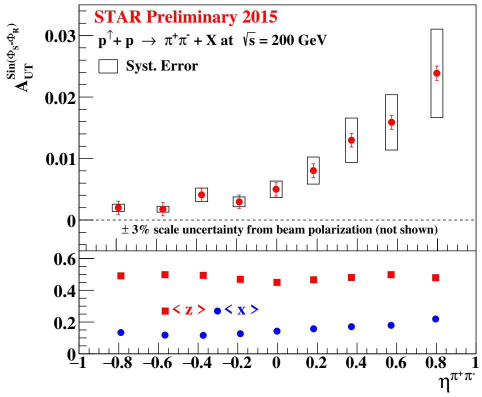

Fig. 4. $A_{UT}^{sin(\phi_{RS})}$ as a function of $\eta^{\pi^+\pi^-}$, integrated over $M_{inv}^{\pi^+\pi^-}$ and $p_T^{\pi^+\pi^-}$ (*top panel*). The quark $\langle z\rangle$ and $\langle x\rangle$, in the corresponding $\eta^{\pi^+\pi^-}$ bins, are shown in the *bottom panel*.

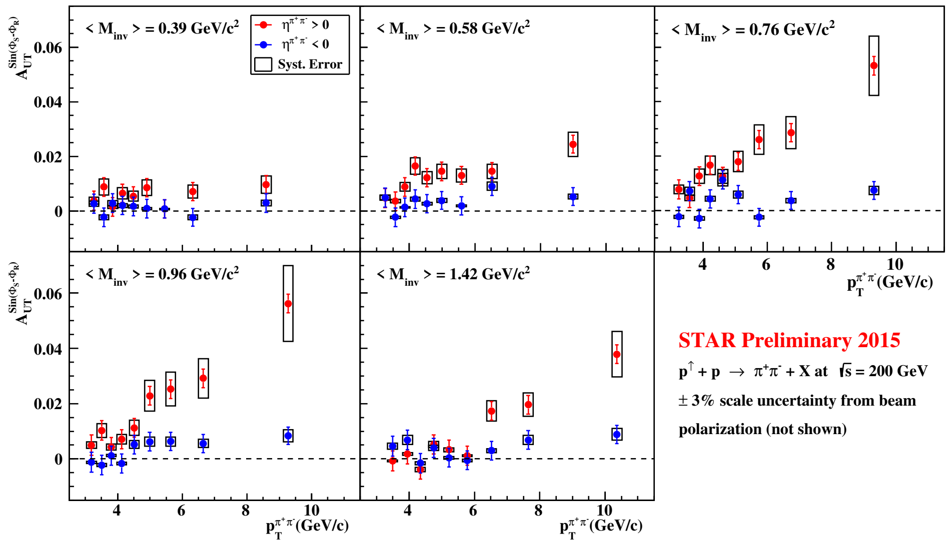

Fig. 5. $A_{UT}^{sin(\phi_{RS})}$ vs $p_T^{\pi^+\pi^-}$, in five $M_{inv}^{\pi^+\pi^-}$ bins in $\eta^{\pi^+\pi^-} > 0$ and $\eta^{\pi^+\pi^-} < 0$ regions. The value of $\langle M_{inv}^{\pi^+\pi^-}\rangle$ for each of the invariant mass bins is shown at the top left corner of each panel.

$A_{UT}^{sin(\phi_{RS})}$ as a function of $p_T^{\pi^+\pi^-}$ in five $M_{inv}^{\pi^+\pi^-}$ bins in forward (*in red*) and backward (*in blue*) regions are shown in figure 5. The asymmetry signal rises linearly with the $p_T^{\pi^+\pi^-}$ in the forward region and the trend is much stronger in the invariant mass bin when $\langle M_{inv}^{\pi^+\pi^-}\rangle \sim M_\rho$. The backward asymmetry signal follows a similar trend as in the forward region, however, the amplitude is relatively small.

5. Summary and Outlook

STAR has measured di-pion correlation asymmetries through the IFF channel based on 2015 $p^{\uparrow}p$ data at $\sqrt{s} = 200$ GeV. This dataset covers the Q^2 at the order of ~ 100 GeV^2 at intermediate x, which is well within the valance quark region. The measured IFF asymmetry signal is enhanced around $M_{inv}^{\pi^+\pi^-} \sim 0.8$ GeV$/c^2$, which is consistent with the theoretical calculation and the previous STAR measurements. A large asymmetry in the forward $\eta^{\pi^+\pi^-}$ region corresponds to higher x, where quark transversity is expected to be sizeable, whereas the backward asymmetries are small, since they probe polarized low-x quarks and scattered quarks from the unpolarized beam. The statistical precision of these results is largely improved compared to the previous STAR results. The systematic uncertainty includes the effect of the PID and trigger bias. The large systematic uncertainty is dominated by the PID effect, which will be better understood and reduced in the near future using the TOF PID information. These high-precision IFF asymmetry results will help to constrain the valance-quark transversity distributions. They will further test the universality of the mechanism producing such asymmetries in different collision processes: SIDIS, e^+e^-, and $p^{\uparrow}p$.

References

[1] H. Abramowicz et al., Eur. Phys. J. C **75**(12), 580 (2015).
[2] D. de Florian, R. Sassot, M. Stratmann and W. Vogelsang, Phys. Rev. D **80**, 034030 (2009).
[3] Z.-B. Kang, A. Prokudin, P. Sun and F. Yuan, Phys. Rev. D **93**, 014009 (2016).
[4] K. H. Ackermann et al., Nucl. Instrum. Meth. A **499**, 624 (2003).
[5] W. Llope, Nucl. Instrum. Meth. **241**(1), 306 (2005).
[6] L. Adamczyk et al. [STAR Collaboration], Phys. Rev. Lett. **115**, 242501 (2015).
[7] L. Adamczyk et al. [STAR Collaboration], Phys. Lett. B **780**, 332 (2018).
[8] G. G. Ohlsen and P. Keaton, Nucl. Instrum. Meth. **109**(1), 41 (1973).
[9] Bacchetta et al., Phys. Rev. D **70**(9) (2004).
[10] Sjostrand et al., Journal of High Energy Phys. **2006**(05), 026-026 (2006)
[11] R. Brun et al., CERN, Geneva (1978).
[12] A. Bacchetta and M. Radici, Phys. Rev. D **67**, 094002 (2003).
[13] M. Radici, Private communication.